Eu^{3+} doped high-brightness fluorophosphate laser-driven glass phosphors

WANG, B.; LI, D. S.; SHEN, L. F.; PUN, E. Y. B.; LIN, H.

Published in:
Optical Materials Express

Published: 01/04/2019

Document Version:
Final Published version, also known as Publisher's PDF, Publisher's Final version or Version of Record

Published version (DOI):
10.1364/OME.9.001749

Publication details:
WANG, B., LI, D. S., SHEN, L. F., PUN, E. Y. B., & LIN, H. (2019). Eu^{3+} doped high-brightness fluorophosphate laser-driven glass phosphors. *Optical Materials Express*, *9*(4), 1749-1762. Article 355437. https://doi.org/10.1364/OME.9.001749

Research Article | Vol. 9, No. 4 | 1 Apr 2019 | OPTICAL MATERIALS EXPRESS 1749
Optical Materials EXPRESS

Eu^{3+} doped high-brightness fluorophosphate laser-driven glass phosphors

B. WANG,[1] D. S. LI,[1] L. F. SHEN,[2,3] E. Y. B. PUN,[2] AND H. LIN[1,2,*]

[1]*School of Information Science and Engineering, Dalian Polytechnic University, Dalian 116034, China*
[2]*Department of Electronic Engineering and State Key Laboratory of Terahertz and Millimeter Waves, City University of Hong Kong, Tat Chee Avenue, Kowloon, Hong Kong, China*
[3]*School College of Microelectronics and Key Laboratory of Optoelectronics Technology, Faculty of Information Technology, Beijing University of Technology, Beijing 100124, China*
**lhai8686@yahoo.com*

Abstract: High-brightness orangish red fluorescence emissions were captured in Eu^{3+} doped fluorophosphate (NBFP) glasses with outstanding rare earth (RE) ion solubility under laser excitation. Highly efficient emissions of Eu^{3+} doped NBFP glasses in the wavelength range of 580–720 nm make the phosphors potential candidates as a remarkable orangish red lighting source. The net emission power and the net emission photon number in 6.0wt% Eu_2O_3 doped NBFP glass were derived to be 6.48 mW and 2.08×10^{16} cps under the excitation of 465 nm laser with 53.46 mW optical power, respectively, and total measured quantum yield was as high as 54.03%. When the excitation power was increased to 561 mW, the luminous flux of 6.0wt% Eu_2O_3 doped NBFP glass was up to 31.21 lm, demonstrating that Eu^{3+} heavy-doped NBFP glasses are potential lighting source materials. Thus, the laser-driven high-brightness phosphors originating from the sufficient photon release of Eu^{3+} ions promote further development of orangish red lighting source.

1. Introduction

Laser-driven rare earth (RE) ions doped glass phosphors are potential illumination materials due to their long fluorescence lifetime, high brightness, and lower energy consumption [1,2]. With the commercialization of visible laser sources, the research of RE^{3+} ions (Dy^{3+}, Sm^{3+}, Tm^{3+}, Eu^{3+}, Pr^{3+}) doped glasses are promoted [3–7]. Among the RE ions, Eu^{3+} as a desirable activator for numerous hosts has been considered as an excellent luminescent center because of its efficient $^5D_0 \rightarrow {}^7F_2$ transition and heavy-doped characteristic. Moreover, Eu^{3+} heavy-doped glasses can release high-brightness orangish-red fluorescence to serve in various fields, such as medical diagnostics, solid-state laser lighting, emissive displays and other applications [8–14]. In particularly, Eu^{3+} ions exhibit admirable high-brightness fluorescence at 590–720 nm wavelength, which is situated in the maximum absorption regions of the photosensitizer currently employed in therapy and clinical trials. Thus, the exploration focusing on high-bright Eu^{3+} heavy-doped glasses driven by laser becomes urgent.

For Eu^{3+} doped glass phosphors, fluorophosphate glasses are promising candidates for photoluminescence materials due to their outstanding RE ions solubility, high transmittance, excellent thermal stability and high laser-damage threshold [15–25]. Furthermore, the fluoride in fluorophosphate glasses effectively reduces the presence of hydrogen and hydroxyl ions, which generates stronger fluorescent emission of RE ions [26–28]. In order to obtain high brightness in glass phosphors, laser-driven approach is employed due to its advantages of strong optical coherence and accurate emission wavelength [29]. In addition to this, the residual laser can be easily filtered out by the short-wave cut-off filter [30].

In this work, transparent Eu^{3+} heavy-doped fluorophosphate glasses (NBFP) were fabricated and characterized. High concentration Eu^{3+} ion and strong applicability host composition contribute to the generation of high-brightness orangish red fluorescence under

#355437 https://doi.org/10.1364/OME.9.001749
Journal © 2019 Received 17 Dec 2018; revised 21 Feb 2019; accepted 21 Feb 2019; published 13 Mar 2019

Optical Materials EXPRESS

the excitation of 465 nm laser excitation. A low non-radiative relaxation rate was identified and internal quantum yield of over 96% was derived from the lifetime analysis in the case when the Eu_2O_3 concentration is less than 6.0 wt%, providing an effective approach for synthesizing heavy-doped RE fluorescent material. In addition, the emission power and the measured quantum yield were calculated to be 6.48 mW and 54.03% under the excitation of 465 nm laser with 53.46 mW optical power, respectively. Furthermore, 31.21lm radiation luminous flux was obtained in 6.0wt% Eu_2O_3 doped NBFP glass when the excitation power was increased to 561mW, which was bright enough to become a practical material for light sources. These results indicate that high-bright orangish red NBFP glass phosphors are promising candidates to develop illumination devices.

2. Materials and experiments

Eu^{3+} heavy-doped NBFP glasses were prepared from high-purity $NaPO_3$, BaF_2 and Eu_2O_3 according to the molar composition of $37.5Na_2O$-$25BaF_2$-$37.5P_2O_5$, In addition, 0.2wt%, 0.5wt%, 1.0wt%, 2.0wt%, 4.0wt% and 6.0wt% Eu_2O_3 as dopants were adopted in NBFP glasses based on the host glass weights, respectively. Firstly, the well-mixed raw materials in alumina crucibles were put into electric furnace, then melted at 930 °C for 40 min. Secondly, the melts were poured into an aluminum mold for quenching and forming. Finally, the glasses were annealed at 390–400 °C for 8 h in order to remove residual stresses within the glasses, and after that cooled down slowly to room temperature. For further optical measurements, the glass samples were sliced and polished into the pieces with two parallel sides.

Using the Metricon 2010 prism coupler, the refractive indices of 2.0wt% Eu_2O_3 doped NBFP glass were measured to be 1.5479 and 1.5342 at 635.96 and 1546.9 nm, respectively, the refractive indices of the glass samples at other wavelengths were obtained by the Cauchy's equation $n = A + B/\lambda^2$ with A = 1.5314 and B = 6668 nm^2 [31]. The density of NBFP glass with 2.0wt% Eu_2O_3 was measured to be 3.31 g/cm^3 by Archimedes method, and thus the number density of Eu^{3+} ions was calculated to be 2.22×10^{20} cm^{-3}. Emission and excitation spectra were recorded by a Hitachi F-7000 fluorescence spectrophotometer, which were corrected with Rhodamine B method. The optical transmission spectrum was presented by a Lambda 950 spectrophotometer. The spectral resolutions for optical transmission and visible spectra are 0.05 nm and 1.0 nm, respectively. The X-ray diffraction (XRD) pattern spectrum was obtained by a Shimadzu XRD-7000 (Cu-Ka, 40 kV, 30 mA) diffractometer. Differential scanning calorimetry (DSC) was measured by using American TA company SDT-600 with the rate of 10 °C/min from room temperature to 800°C under N_2 atmosphere (flow of 100 ml/min). Fluorescence decay curves were measured by a Jobin Yvon Fluorolog-3 spectrophotometer equipped with an R928 photomultiplier tube (PMT) detector, and a pulsed Xenon-lamp was adopted as the pump source. The absolute spectral parameters were obtained in a 25 cm inner diameter integrating sphere (Labsphere) which was connected to a QE65000 CCD detector (Ocean Optics) with a 600 μm-core optical fiber. A 465 nm diode laser were adopted as pumping source, and detailed optical powers in operating processes are presented in the following text. A standard SCL-050 halogen lamp (Labsphere) was employed for calibrating the measurement system. All the experiments were carried out at room temperature.

3. Results and discussion

3.1 Radiative transition properties of Eu^{3+} doped NBFP glasses

The normalized emission spectra of Eu_2O_3 doped NBFP glasses with different Eu^{3+} concentration are recorded under 395 nm excitation as shown in Fig. 1. The seven emission peaks are located at 537, 555, 579, 592, 615, 653 and 702 nm, respectively, which originate from the different excited levels of Eu^{3+} to the lower levels ^7F_J (J = 0,1, 2, 4) transitions [32–

Optical Materials EXPRESS

34]. Among them, the $^5D_0 \rightarrow {}^7F_2$ electric dipole transition at 615 nm is a more hypersensitive transition than others [35,36]. In the inset of Fig. 1, the brightness of the glass phosphors has an obvious upgrade with the increasing amount of Eu^{3+} ions in the clockwise direction, confirming the emission intensity is proportional to Eu_2O_3 doping concentration.

The normalized excitation spectra of Eu^{3+} doped NBFP glasses monitored at 615 nm are exhibited in Fig. 2. The spectra consist of ten excitation bands peaking at 252, 287, 299, 320, 362, 383, 395, 416, 466 and 527 nm. The broad charge transfer bands (CTS) in UV region located between 205 nm and 283 nm, which is due to the electron transition from O^{2-} to $^4f_6$ shell of Eu^{3+} ions [37], and other excitation bands are owing to the 4f–4f inner shell transitions of Eu^{3+} ions. The presence of widespread excitation bands indicates orangish red fluorescence can be achieved by UV/violet/blue/green laser pumping. Although the most efficient excitation wavelength is 395 nm in the glass system, 465 nm commercial laser is chosen as excitation source from the pratical perspective to pump orangish red light source materials in industrial development. The relationship between emission intensity and Eu_2O_3 doping concentration has been fitted, and intensity in high doping (>6wt%) cases are anticipated in the inset of Fig. 2. The concentration quenching in Eu^{3+}-doped NBFP glasses is considered to occur at about 9.0wt% Eu_2O_3 doping.

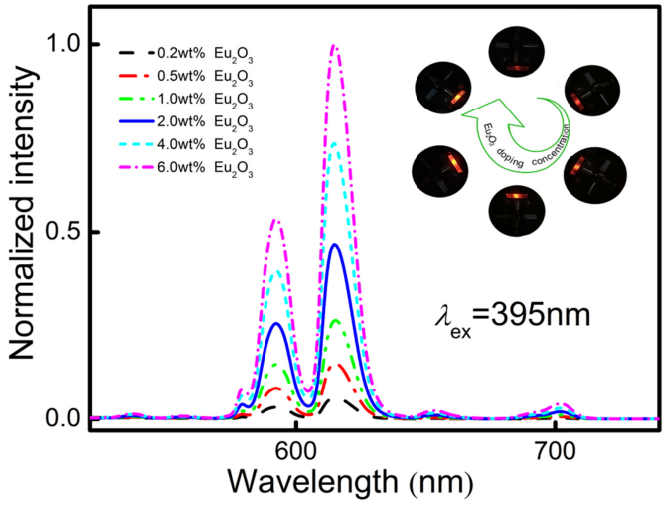

Fig. 1. Normalized emission spectra of 0.2wt%, 0.5wt%, 1.0wt%, 2.0wt%, 4.0wt% and 6.0wt% Eu_2O_3 doped NBFP glasses under 395 nm excitation. Inset: fluorescent photographs with increasing dopant concentration in the clockwise direction under 395 nm excitation.

Optical Materials EXPRESS

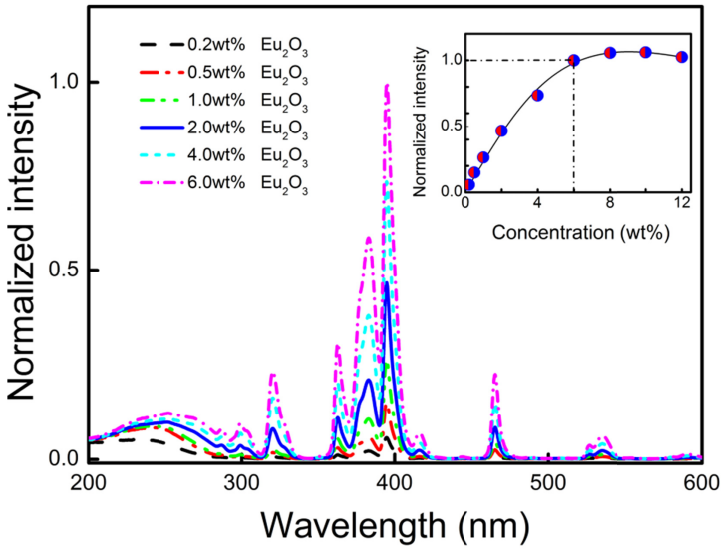

Fig. 2. Normalized excitation spectra of 0.2wt%, 0.5wt%, 1.0wt%, 2.0wt%, 4.0wt% and 6.0wt% Eu_2O_3 doped NBFP glasses monitoring at 615 nm emission. Inset: the relationship between emission intensity and Eu_2O_3 doping concentration.

3.2 Properties of thermodynamics and transmittance in Eu^{3+} doped NBFP glasses

The X-ray diffraction (XRD) pattern spectrum of 2.0wt% Eu_2O_3 doped NBFP glass exhibits two broad peaks and no sharp diffraction peak in Fig. 3, which indicates that the NBFP glasses system is an amorphous state. Moreover, the thermodynamic properties of 6.0wt% Eu_2O_3 doped NBFP glass are exhibited by DSC curve in Fig. 3(a). The transition temperature (T_g), the crystallization onset temperature (T_x) and the crystallization temperature (T_c) of Eu^{3+} heavy-doped NBFP glass were identified as 403 °C, 544 °C and 570 °C, respectively. The temperature difference values ($\Delta T = T_x - T_g$) should be as large as possible to be considered as good optical glasses, and a ΔT value larger than 100 °C suggests excellent glass thermodynamic stability [38]. The ΔT of NBFP glass is calculated to be 141 °C, demonstrating the sample exhibits good stability when 6.0wt% Eu_2O_3 is heavily doped. Besides, in Fig. 3(b) Eu_2O_3 doped NBFP glass presents 80% transmittance in addition to the strong absorption bands of Eu^{3+} located at 300–403 nm and 1889–2246 nm in the transmission spectrum, indicating the energy of laser can be efficiently absorbed by RE ions, and the photon of Eu^{3+} can be adequately released. Thus, Eu^{3+} doped NBFP glasses with excellent transmittance and well thermodynamic stability are good candidates for illumination devices.

Optical Materials EXPRESS

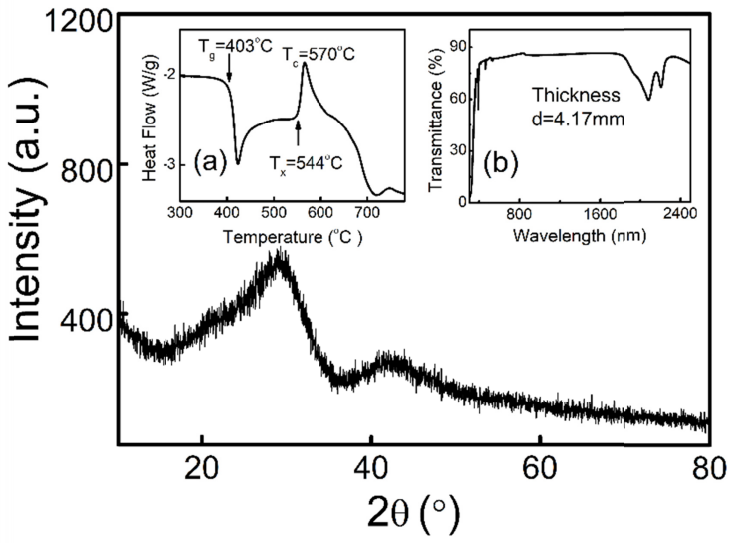

Fig. 3. XRD pattern spectrum of 2.0wt% Eu_2O_3 doped NBFP glass. Insets: DSC curve of 6.0wt% doped NBFP glass (a) and optical transmission spectrum of 2.0wt% Eu_2O_3 doped NBFP glass (b).

3.3 Quantitative characterization and brightness analysis of Eu^{3+} doped NBFP glasses

Absolute spectral parameters are obtained by the integrating sphere coupled with a CCD detector, providing measured quantum yield QY_M to evaluate luminescence prospect of laser-driven light source materials [39]. As shown in Fig. 4, the net spectral power distributions are obtained for 2.0wt% and 6.0wt% Eu_2O_3 doped NBFP glasses under 465 nm laser excitation. Here, the spectral power distribution curves consist of six emission bands located at 579, 592, 614, 653, 701 and 804 nm, which are attributed to $^5D_0 \rightarrow {}^7F_0$, $^5D_0 \rightarrow {}^7F_1$, $^5D_0 \rightarrow {}^7F_2$, $^5D_0 \rightarrow {}^7F_3$, $^5D_0 \rightarrow {}^7F_4$, and $^5D_0 \rightarrow {}^7F_6$ transitions, respectively. The net emission powers of 2.0 wt% Eu_2O_3 doped NBFP glass are derived to be 1.25 and 2.72 mW under the excitation of 465 nm laser with of 25.19 and 53.46 mW optical powers, respectively. In addition, the corresponding net emission powers of 6.0 wt% Eu_2O_3 doped NBFP glass are as high as 2.99 and 6.48 mW under the 25.19 and 53.46 mW, respectively, revealing that heavy-doped Eu^{3+} ions and high laser power contribute to more intense orangish red emission. The color of the fluorescent changes from magenta to orangish red as exhibited in the inserted photographs of Fig. 4 with the increasing emission power of Eu^{3+} doped NBFP glasses.

In this work, the net photon distribution is derived by the equation

$$N(v) = \frac{\lambda^3}{hc} P(\lambda), \tag{1}$$

in which v is the wavenumber, c is the vacuum light velocity, h is the Planck constant, and $P(\lambda)$ is the net spectral power distribution [40]. As presented in Fig. 5, absorption and emission photon distributions of Eu^{3+} doped NBFP glasses are derived from Eq. (1) with corresponding $P(\lambda)$. The absorption and emission photon numbers of these phosphors have been deduced and summarized in Table 1, and relevant results reveal that the Eu^{3+} ions doped NBFP glass system has outstanding photoluminescence behavior and excellent absorption capacity for the 465 nm laser beam.

Optical Materials EXPRESS

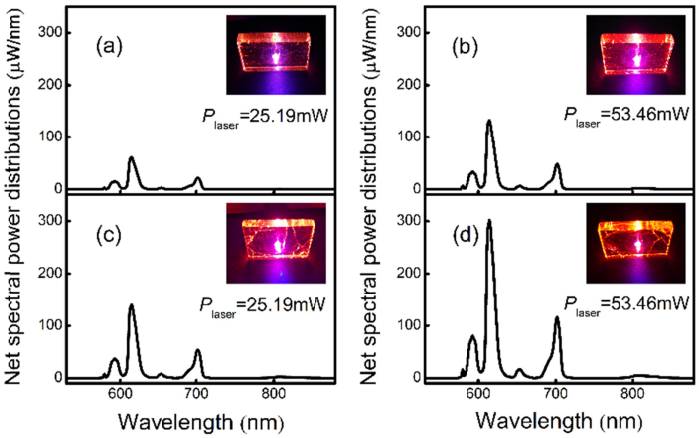

Fig. 4. Net spectral power distribution curves of 2.0wt% (a-b) and 6.0wt% (c-d) Eu_2O_3 doped NBFP glasses under 465 nm laser excitation with different power. Insets: fluorescent photographs of 2.0wt% (a-b) and 6.0wt% (c-d) Eu_2O_3 doped NBFP glasses under 465 nm laser excitation with different power.

The measured quantum yield is a selection criterion for assessing the effectiveness of photoluminescence materials for orangish red light sources, which is defined as the ratio of the number of emitted photons N_{em} to that of absorbed photons N_{abs}

$$QY_M = N_{em} / N_{abs} \quad (2)$$

All the QY_M values of $^5D_0 \rightarrow {}^7F_J$ (J = 0, 1, 2, 3, 4, 6) transition emissions for Eu^{3+} doped NBFP glasses have been obtained and listed in Table 1. The total QY_M values vary from ~40% to ~54% when Eu^{3+} ions doping concentrations increase from 2.0wt% to 6.0wt%. The total QY_M for 6.0wt% Eu_2O_3 heavy-doped NBFP glass is no less than 50% when optical power is adjusted from 25.19 to 53.46 mW. The total QY_M for 6.0wt% Eu_2O_3 doped NBFP glass is larger than 9% in MoO_3–ZnO–B_2O_3 crystallized glass [41], 13.4% in BaF_2–SrF_2–AlF_3–YF_3–$Al(PO_3)_3$ glass [42] and 3.2% in GaN layers [43]. Besides, the absorption coefficient 0.076 cm^{-1} for $^7F_0 \rightarrow {}^5D_2$ in the 2.0wt% Eu_2O_3 doped NBFP glass is superior to ~0.04 cm^{-1} in Eu_2O_3 doped $Li_2B_4O_7$ glass [44], and in the perspective of photon release, the QY_M of 2.0 wt% Eu_2O_3 doped NBFP glass is 40.74%, which is higher than 10.6% in $Li_2B_4O_7$ glass. Thus, the Eu^{3+} heavy-doped NBFP glasses are preeminent candidates for 465nm laser driven materials in orangish red light source.

Optical Materials EXPRESS

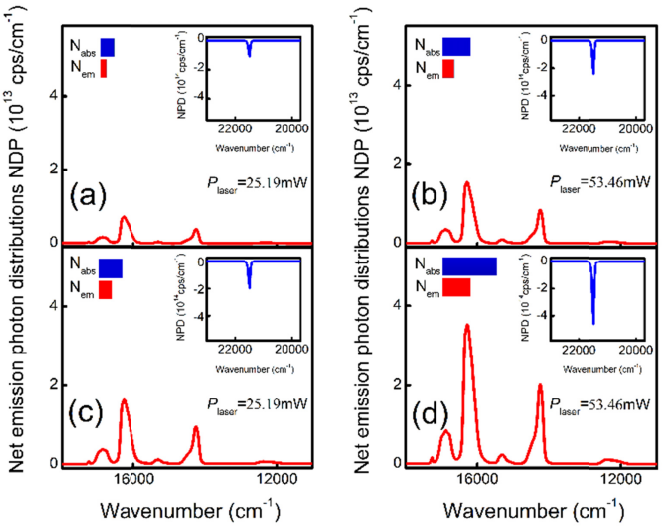

Fig. 5. Net emission photon distributions in 2.0wt% (a-b) and 6.0wt% (c-d) Eu_2O_3 doped NBFP glasses under the excitation 465 nm laser with different power. Inset: net absorption photon distributions under the 465 nm laser excitation, the area of red and blue rectangles stand for absorption and emission photon numbers, respectively.

Table 1. Absorption and emission photon numbers and measured quantum yields in Eu^{3+} doped NBFP glasses under 465 nm laser excitation.

Eu_2O_3 concentration (wt%)	Excitation power (mW)	N_{abs} (10^{14} cps)	N_{em} (10^{14} cps)	QY_M (%)
2.0wt% (Size: 23.92 × 15.32 × 4.17 mm^3)	25.19	100.87	40.01	39.66
	53.46	213.71	87.07	40.74
6.0wt% (Size: 24.65 × 15.76 × 3.81mm^3)	25.19	177.27	95.78	54.03
	53.46	400.88	207.73	51.82

Judd–Ofelt (J–O) intensity parameters Ω_t (t = 2, 4, 6) are important indicators to evaluate the interaction between RE ion and host [45–47]. Intensity parameters are listed in Table 2, and Ω_2 is obtained to be 7.461 × 10^{-20} cm^2, which shows the higher asymmetry and the stronger covalency around Eu^{3+} ions. The presence of fluoride is beneficial for improving the Eu^{3+} ions solubility in the NBFP glasses. The Ω_4 and Ω_6 are calculated to be 6.687 × 10^{-20} and 1.507 × 10^{-20} cm^2, respectively, which indicate the vibronic transitions of the Eu^{3+} ion-ligand bond and reflect the acid-basicity and the rigidity of NBFP glasses. Spontaneous transition probabilities A_{ij}, branching ratios β_{ij}, and the radiative lifetimes τ_{rad} of $^5D_0$ level of 2.0wt% Eu_2O_3 doped NBFP glass are derived and shown in Table 3. The A_{ij} of the $^5D_0 \rightarrow {}^7F_J$ (J = 1, 2, 4, 6) transitions are obtained to be 63.74, 248.30, 106.36 and 1.34 s^{-1}, respectively. The fluorine ions in the glass induce structural changes in the vicinity of the Eu^{3+} ions, which in turn decrease the electronic transition probabilities leading to an increase in lifetimes of the $^5D_0$ level. The β_{ij} are calculated to be 15.19%, 59.16%, 25.33% and 0.32% for $^5D_0 \rightarrow {}^7F_J$ (J

Optical Materials EXPRESS

= 1, 2, 4, 6) transitions, respectively, predicting the efficient orangish red emissions of Eu^{3+} ions satisfy some special demands.

Table 2. Photon number ratios and intensity parameters (Ω_2, Ω_4 and Ω_6) in Eu^{3+} doped NBFP glasses under 465 nm laser excitation.

Transitions	Energy (cm^{-1})	Photon number ratio	J–O intensity parameter ($10^{-20}cm^2$)
$^5D_0 \rightarrow {}^7F_1(N_1)$	16874	–	–
$^5D_0 \rightarrow {}^7F_2(N_2)$	16279	$N_2/N_1 = 3.896$	$\Omega_2 = 7.461$
$^5D_0 \rightarrow {}^7F_4(N_4)$	14248	$N_4/N_1 = 1.668$	$\Omega_4 = 6.687$
$^5D_0 \rightarrow {}^7F_6(N_6)$	12320	$N_6/N_1 = 0.210$	$\Omega_6 = 1.507$

Table 3. Spontaneous transition probabilities A_{ij}, branching ratios β_{ij} and radiative fluorescent lifetime τ_{rad} of $^5D_0$ level in Eu^{3+} doped NBFP glasses.

Transition	Energy (cm^{-1})	A_{ij} (s^{-1})	β_{ij} (%)	τ_{rad} (ms)
$^5D_0 \rightarrow {}^7F_1$	16874	63.74	15.19	2.38
$^5D_0 \rightarrow {}^7F_2$	16279	248.30	59.16	
$^5D_0 \rightarrow {}^7F_4$	14248	106.36	25.33	
$^5D_0 \rightarrow {}^7F_6$	12320	1.34	0.32	

Fluorescence decay curves of $^5D_0$ level in Eu^{3+} doped NBFP glasses monitoring at 615 nm under 465 nm laser excitation are presented in Fig. 6. The experimental average lifetime $\tau_{exp\text{-}avg}$ of the $^5D_0$ level for Eu^{3+} doped NBFP glass can be derived from the fluorescence decay curves using the following equation

$$\tau_{exp-avg} = \frac{\int_0^\infty tI(t)\,dt}{\int_0^\infty I(t)\,dt}, \quad (3)$$

where $I(t)$ is the emission intensity [48,49]. The related results are calculated and listed in Table 4. The $\tau_{exp\text{-}avg}$ are obtained to be 2.36, 2.34, 2.32 and 2.29 ms for 0.2wt%, 2.0wt%, 4.0wt% and 6.0wt% Eu_2O_3 doped NBFP glass samples, respectively, indicating the effect of Eu^{3+} concentration on the $\tau_{exp\text{-}avg}$ in NBFP glass system is not significant. Based on the $\tau_{exp\text{-}avg}$ and τ_{rad}, the lifetime-based quantum yields QY_L of the $^5D_0$ level for the NBFP glasses in the visible region can be obtained by $QY_L = \tau_{exp\text{-}avg}/\tau_{rad}$, the QY_L of 0.2wt%, 2.0wt%, 4.0wt% and 6.0wt% Eu_2O_3 doped NBFP glasses are up to be 99.2%, 98.3%, 97.5% and 96.2%,

Optical Materials EXPRESS

respectively, and the variation of QY_L displays an extremely slow decrease tendency with the increasing of Eu^{3+} ions.

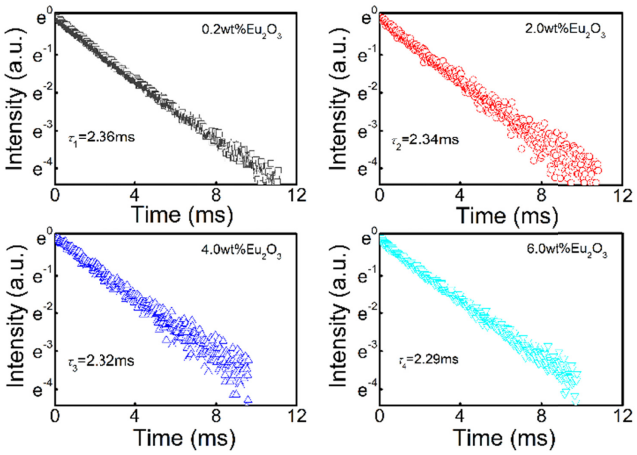

Fig. 6. Fluorescence decay curves of 0.2wt%, 2.0wt%, 4.0wt% and 6.0wt% Eu_2O_3 doped NBFP glasses monitoring at 615 nm under 465 nm laser excitation.

Non-radiative relaxation rate W_{NR} includes multi-phonon relaxation W_{MPR} rate and cross relaxation rate W_{CR}. When the lowest concentration 0.2wt% Eu_2O_3 is adopted, the cross relaxation behavior is negligible, thus, W_{MPR} can be calculated by the following equation

$$1/\tau_{exp-avg} = 1/\tau_{rad} + W_{MPR} + W_{CR} \quad (4)$$

[50]. Furthermore, the cross relaxation rates for other Eu_2O_3 doped NBFP glasses are derived by substituting the W_{MPR} into Eq. (4). The corresponding parameters $\tau_{exp-avg}$, QY_L, W_{CR}, and W_{MPR} are listed in Table 4 for various Eu^{3+} doped glasses. The ~17 s^{-1} W_{NR} value of 6.0wt% Eu_2O_3 doped glass is lower than 61 s^{-1} in P_2O_5–K_2O–Al_2O_3–PbF_2–Na_2O glass [51], 272 s^{-1} in PbF_2–TeO_2–H_3BO_3 glass [52], 289 s^{-1} in TeO_2–La_2O_3–$10TiO_2$ glass [53]. The low W_{NR} rate indicates there is ultrahigh concentration quenching even if Eu^{3+} ions are adequately heavily doped in NBFP glasses.

Table 4. Experimental average fluorescent lifetimes $\tau_{exp-avg}$, lifetime-based quantum yield QY_L values, multi-phonon relaxation rates W_{MPR} and cross relaxation rates W_{CR} of Eu^{3+} doped NBFP glasses.

Eu_2O_3 concentration (wt%)	$\tau_{exp-avg}$ (ms)	QY_L (%)	W_{MPR} (s^{-1})	W_{CR} (s^{-1})
0.2	2.36 ± 0.01	99.2	3.56	–
2.0	2.34 ± 0.01	98.3	3.56	3.62
4.0	2.32 ± 0.01	97.5	3.56	7.31
6.0	2.29 ± 0.01	96.2	3.56	12.95

For the potential illumination material, the characterization of absolute spectral parameter under laser pumping is essential to assess practical level of photoluminescence materials [54–56]. As shown in Fig. 7, the net spectral power distributions for 2.0wt% and 6.0wt% Eu_2O_3

Optical Materials EXPRESS

doped NBFP glasses were obtained when 465 nm laser optical power was incresed 561 mW. Meanwhile, the corresponding net emission spectral powers for Eu_2O_3 doped NBFP glasses were up to 52.67 and 116.52 mW under 465 nm laser excitation, respectively. The peak position and shape of the net spectral power distributions are as same as the spectral characteristic of Fig. 4. However, the net emission power for 6.0wt% Eu_2O_3 doped glass is above 18 times than that of Fig. 4(d).

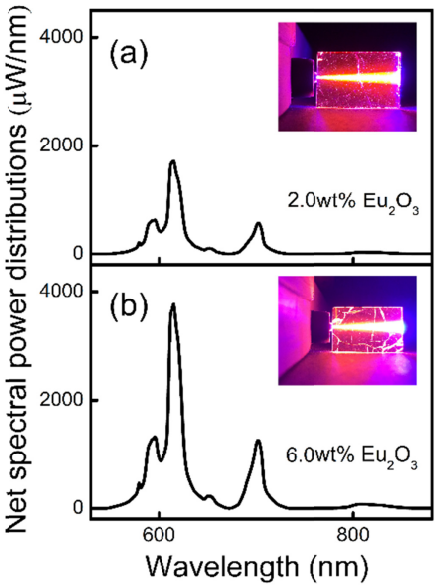

Fig. 7. Net spectral power distributions for 2.0wt% and 6.0wt% Eu_2O_3 doped NBFP glasses under 465 nm laser excitation with 561 mW power. Insets: fluorescent photographs of 2.0wt% and 6.0wt% Eu_2O_3 doped NBFP glasses under 465 nm laser excitation with 561 mW.

Optical Materials EXPRESS

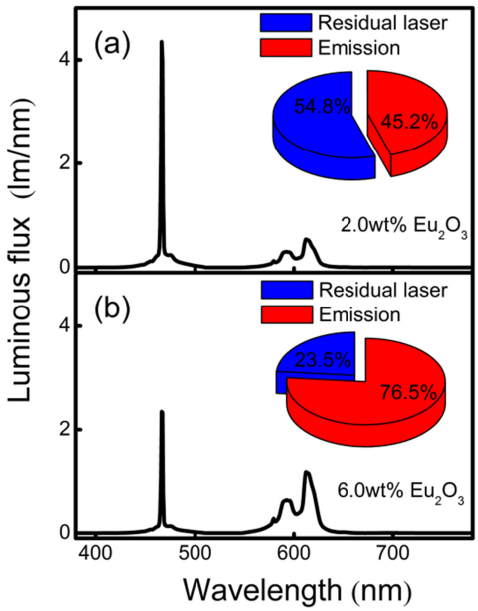

Fig. 8. Luminous flux distributions of 2.0wt% and 6.0wt% Eu_2O_3 doped NBFP glasses under 465 nm laser excitation with 561 mW power. Insets: pie charts display the percentage of the luminous fluxes between the orangish red emission and those of residual laser.

Luminous flux is defined as a derived quantity from radiant flux by evaluating the radiation power that based on its perception upon the standard photometric observer. As presented in Fig. 8, the total luminous fluxes Φ_V of the material are deduced under 465 nm laser excitation with 561 mW power by the equation

$$\Phi_V = K_m \int_{380}^{780} V(\lambda) P(\lambda) d\lambda, \quad (5)$$

where Φ_V is the luminous flux, $V(\lambda)$ is relative eye sensitivity, and K_m is the maximum luminous efficacy at 555 nm (683 lm/W) [57–59]. The luminous flux distributions of the 2.0wt% and 6.0wt% Eu_2O_3 doped NBFP glasses are presented in Fig. 8 under the excitation of 465 nm laser with 561 mW optical power, and relevant results are summarized in Table 5. The pie charts display the increase of the emission luminous fluxes and the decline of residual laser luminous flux by increasing Eu_2O_3 doping concentration, providing a high-efficient approach to improve usage of the 465 nm laser by adopting Eu^{3+} heavy-doped NBFP glasses. The total emission luminous fluxes of 2.0wt% and 6.0wt% Eu_2O_3 doped NBFP glasses are 14.27 and 31.21 lm. The Eu_2O_3 heavy-doped NBFP glass with 31.21 lm luminous flux is bright enough to be a practical light source, further demonstrating its potential as illumination material.

Optical Materials EXPRESS

Table 5. Emission luminous fluxes, residual laser luminous fluxes, and total luminous fluxes from 2.0wt% and 6.0wt% Eu_2O_3 doped NBFP glass under the excitation of 465 nm laser with 561 mW power.

Eu_2O_3 concentration (wt%)	Emission luminous flux (lm)	Residual laser luminous flux (lm)	Total luminous flux (lm)
2.0	14.27	17.28	31.55
6.0	31.21	9.61	40.82

4. Conclusion

Eu^{3+} heavy-doped fluorophosphate glass (NBFP) phosphors were prepared, and the high-brightness orangish red fluorescence exhibits their potential as light source. Low non-radiative relaxation rate contributes to the lifetime-based quantum yield of over 96% and ultrahigh concentration quenching in the Eu^{3+} heavy-doped fluorescent material. The net emission power and the net emission photon number in 6.0wt% Eu_2O_3 doped NBFP glass were derived to be 6.48 mW and 2.08×10^{16} cps under 465 nm laser with 53.46 mW optical power pumping, respectively, and measured quantum yield is calculated to be 54.03%. Furthermore, the luminous flux is up to 31.21 lm when the excitation power is increased to 561mW, which can satisfy the essential demands of practical brightness illumination. The high-brightness orangish red fluorescence demonstrates the superiority of laser-driven high-brightness Eu^{3+} heavy-doped NBFP glasses as lighting source, which promotes the further development of orangish red illumination.

Funding

Natural Science Foundation of Liaoning Province, China (Grant No. 20170540068); Research Grants Council of the Hong Kong Special Administrative Region, China (Grant No. CityU 11218018).

References

1. J. Rocha, L. D. Carlos, F. A. A. Paz, and D. Ananias, "Luminescent multifunctional lanthanides-based metal-organic frameworks," Chem. Soc. Rev. **40**(2), 926–940 (2011).
2. M. Ozaki, J. Kato, and S. Kawata, "Surface-plasmon holography with white-light illumination," Science **332**(6026), 218–220 (2011).
3. S. Pleasants, "Animal vision: Colour perception," Nat. Photonics **8**(4), 267 (2014).
4. B. Zhou, B. Shi, D. Jin, and X. Liu, "Controlling upconversion nanocrystals for emerging applications," Nat. Nanotechnol. **10**(11), 924–936 (2015).
5. D. C. Zhou, R. F. Wang, X. J. He, J. Yi, Z. G. Song, Z. W. Yang, X. H. Xu, X. Yu, and J. Qiu, "Color-tunable luminescence of Eu^{3+} in PbF_2 embedded in oxyfluoroborate glass and its nanocrystalline glass," J. Alloys Compd. **621**, 62–65 (2015).
6. S. L. Dong, S. Ye, L. L. Wang, X. Y. Chen, S. B. Yang, Y. J. Zhao, J. G. Wang, X. P. Jing, and Q. Y. Zhang, "$Gd_3B(W,Mo)O_9:Eu^{3+}$ red phosphor: from structure design to photoluminescence behavior and near-UV white-LEDs performance," J. Alloys Compd. **610**, 402–408 (2014).
7. H. Rahimian, Y. Hatefi, A. D. Hamedan, and S. P. Shirmardi, "Structural and optical investigations on Eu 3+ doped fluorophosphate glass and nano glass-ceramics," J. Non-Cryst. Solids **487**, 46–52 (2018).
8. E. G. Rowse, S. Harris, and G. Jones, "The switch from low-pressure sodium to light emitting diodes does not affect bat activity at street lights," PLoS One **11**(3), e0150884 (2016).
9. O. Carrión, A. R. J. Curson, D. Kumaresan, Y. Fu, A. S. Lang, E. Mercadé, and J. D. Todd, "A novel pathway producing dimethylsulphide in bacteria is widespread in soil environments," Nat. Commun. **6**(1), 6579 (2015).
10. F. A. La Sorte, D. Fink, J. J. Buler, A. Farnsworth, and S. A. Cabrera-Cruz, "Seasonal associations with urban light pollution for nocturnally migrating bird populations," Glob. Change Biol. **23**(11), 4609–4619 (2017).
11. T. Cowan and G. Gries, "Ultraviolet and violet light: attractive orientation cues for the indian meal moth, plodia interpunctella," Entomol. Exp. Appl. **131**(2), 148–158 (2009).

Optical Materials EXPRESS

12. J. Rajagukguk, J. Kaewkhao, M. Djamal, R. Hidayat, and Y. Ruangtaweep, "Structural and optical characteristics of Eu^{3+} ions in sodium-lead-zinc-lithium-borate glass system," J. Mol. Struct. **1121**, 180–187 (2016).
13. H. Segawa, N. Hirosaki, S. Ohki, K. Deguchi, and T. Shimizu, "Exploration of metaphosphate glasses dispersed with Eu-doped SiAlON for white LED applications," Opt. Mater. **42**, 399–405 (2015).
14. M. Kemere, J. Sperga, U. Rogulis, G. Krieke, and J. Grube, "Luminescence properties of Eu, RE^{3+} (RE= Dy, Sm, Tb) co-doped oxyfluoride glasses and glass-ceramics," J. Lumin. **181**, 25–30 (2017).
15. M. Zhu, X. Z. Song, S. Y. Song, S. N. Zhao, X. Meng, L. L. Wu, C. Wang, and H. J. Zhang, "A temperature-responsive smart europium metal-organic framework switch for reversible capture and release of intrinsic Eu^{3+} ions," Adv. Sci. (Weinh.) **2**(4), 1500012 (2015).
16. G. Galleani, Y. Ledemi, E. S. de Lima Filho, S. Morency, G. Delaizir, S. Chenu, J. R. Duclere, and Y. Messaddeq, "UV-transmitting step-index fluorophosphate glass fiber fabricated by the crucible technique," Opt. Mater. **64**, 524–532 (2017).
17. R. Balda, J. Fernández, J. L. Adam, and M. A. Arriandiaga, "Time-resolved fluorescence-line narrowing and energy-transfer studies in a Eu^{3+}-doped fluorophosphate glass," Phys. Rev. B Condens. Matter **54**(17), 12076–12086 (1996).
18. R. J. Amjad, M. R. Dousti, M. R. Sahar, S. F. Shaukat, S. K. Ghoshal, E. S. Sazali, and N. Fakhra, "Silver nanoparticles enhanced luminescence of Eu^{3+}-doped tellurite glass," J. Lumin. **154**(1), 316–321 (2014).
19. Q. Zhang, X. F. Liu, Y. B. Qiao, B. Qian, P. D. Guo, J. Ruan, Q. L. Zhou, J. R. Qiu, and D. P. Chen, "Reduction of Eu^{3+} to Eu^{2+} in Eu-doped high silica glass prepared in air atmosphere," Opt. Mater. **32**(3), 427–431 (2010).
20. G. H. Liu, J. T. Li, and L. Wu, "Preparation and optical properties of Eu-doped Y_2O_3–Al_2O_3–SiO_2 glass," Mater. Res. Bull. **48**(10), 3934–3938 (2013).
21. G. Chu, X. S. Wang, T. R. Chen, W. Xu, Y. Wang, H. W. Song, and Y. Xu, "Chiral electronic transitions of YVO_4: Eu^{3+} nanoparticles in cellulose based photonic materials with circularly polarized excitation," J. Mater. Chem. C Mater. Opt. Electron. Devices **3**(14), 3384–3390 (2015).
22. X. Li, H. Zhong, B. Chen, G. Sui, J. Sun, S. Xu, L. Cheng, and J. Zhang, "Highly stable and tunable white luminescence from Ag-Eu^{3+} co-doped fluoroborate glass phosphors combined with violet LED," Opt. Express **26**(2), 1870–1881 (2018).
23. B. J. R. S. Swamy, B. Sanyal, R. Vijay, P. R. Babu, D. K. Rao, and N. Veeraiah, "Influence of copper ions on thermoluminescence characteristics of CaF_2–B_2O_3–P_2O_5, glass system," Ceram. Int. **40**(2), 3707–3713 (2014).
24. K. Binnemans, D. R. Van, C. Gorller-Walrand, and J. L. Adam, "Spectroscopic properties of trivalent lanthanide ions in fluorophosphate glasses," J. Non-Cryst. Solids **238**(1–2), 11–29 (1998).
25. T. Wei, F. Z. Chen, Y. Tian, and Q. S. Xu, "Efficient 2.7 μm emission and energy transfer mechanism in Er^{3+} doped Y_2O_3 and Nb_2O_5 modified germanate glasses," J. Quant. Spectrosc. Ra. **133**, 663–669 (2014).
26. X. Wen, G. Tang, J. Wang, X. Chen, Q. Qian, and Z. Yang, "Tm^{3+} doped barium gallo-germanate glass single-mode fibers for 2.0 μm laser," Opt. Express **23**(6), 7722–7731 (2015).
27. M. Secu, C. E. Secu, and C. Ghica, "Eu-doped CaF_2 nanocrystals in sol-gel derived glass-ceramics," Opt. Mater. **33**(4), 613–617 (2011).
28. V. Vijaya, V. Venkatramu, P. Babu, C. K. Jayasankar, U. R. Rodríguez-Mendoza, and V. Lavín, "Spectroscopic properties of Sm^{3+} ions in phosphate and fluorophosphate glasses," J. Non-Cryst. Solids **365**, 85–92 (2013).
29. T. S. Gonçalves, R. J. M. Silva, M. de Oliveira, Jr., C. R. Ferrari, G. Y. Poirier, H. Eckert, and A. S. S. de Camargo, "Structure-property relations in new fluorophosphate glasses singly-and co-doped with Er^{3+} and Yb^{3+}," Mater. Chem. Phys. **157**, 45–55 (2015).
30. B. D. Wilts, T. M. Trzeciak, P. Vukusic, and D. G. Stavenga, "Papiliochrome II pigment reduces the angle dependency of structural wing colouration in nireus group papilionids," J. Exp. Biol. **215**(Pt 5), 796–805 (2012).
31. R. Zhang, H. Lin, Y. L. Yu, D. Q. Chen, J. Xu, and Y. S. Wang, "A new-generation color converter for high-power white led: transparent Ce^{3+}:YAG phosphor-in-glass," Laser Photonics Rev. **8**(1), 158–164 (2014).
32. H. Gebavi, D. Milanese, R. Balda, M. Ivanda, F. Auzel, J. Lousteau, J. Fernandez, and M. Ferraris, "Novel Tm^{3+}-doped fluorotellurite glasses with enhanced quantum efficiency," Opt. Mater. **33**(3), 428–437 (2011).
33. R. Bagga, V. G. Achanta, A. Goel, J. M. F. Ferreira, N. P. Singh, D. P. Singh, V. Contini, M. Falconieri, and G. Sharma, "Luminescence study of mixed valence Eu-doped nanocrystalline glass–ceramics," Opt. Mater. **36**(2), 198–206 (2013).
34. D. K. Singha, P. Majee, S. K. Mondal, and P. Mahata, "A Eu-doped Y-based luminescent metal-organic framework as a highly efficient sensor for nitroaromatic explosives," Eur. J. Inorg. Chem. **2015**(8), 1390–1397 (2015).
35. H. Guo, X. Wang, J. Chen, and F. Li, "Ultraviolet light induced white light emission in Ag and Eu^{3+} co-doped oxyfluoride glasses," Opt. Express **18**(18), 18900–18905 (2010).
36. P. Adhikary, S. Garain, S. Ram, and D. Mandal, "Flexible hybrid Eu^{3+} doped P(VDF-HFP) nanocomposite film possess hypersensitive electronic transitions and piezoelectric throughput," J. Polym. Sci. Pol. Phys. **54**(22), 2335–2345 (2016).
37. Q. L. Ma, W. S. Yu, X. T. Dong, J. X. Wang, G. X. Liu, and J. Xu, "Electrospinning fabrication and properties of Fe_3O_4/Eu(BA)$_3$phen/PMMA magnetic–photoluminescent bifunctional composite nanoribbons," Opt. Mater. **35**(3), 526–530 (2013).

Optical Materials EXPRESS

38. W. C. Wang, J. Yuan, L. X. Li, D. D. Chen, Q. Qian, and Q. Y. Zhang, "Broadband 2.7 μm amplified spontaneous emission of Er^{3+} doped tellurite fibers for mid-infrared laser applications," Opt. Mater. Express **5**(12), 2964–2977 (2015).
39. S. Fischer, B. Fröhlicha, H. Steinkempera, K. W. Krämerb, and J. C. Goldschmidta, "Absolute upconversion quantum yield of β-$NaYF_4$ doped with Er^{3+} and external quantum efficiency of upconverter solar cell devices under broad-band excitation considering spectral mismatch corrections," Sol. Energy Mater. Sol. Cells **122**(10), 197–207 (2014).
40. C. Würth, M. Grabolle, J. Pauli, M. Spieles, and U. Resch-Genger, "Relative and absolute determination of fluorescence quantum yields of transparent samples," Nat. Protoc. **8**(8), 1535–1550 (2013).
41. L. Aleksandrov, T. Komatsu, R. Iordanova, and Y. Dimitriev, "Structure study of MoO_3–ZnO–B_2O_3 glasses by raman spectroscopy and formation of α-$ZnMoO_4$ nanocrystals," Opt. Mater. **33**(6), 839–845 (2011).
42. T. B. De. Queiroz, M. B. S. Botelho, T. S. Gonçalves, R. Dousti and A. S. S. D. Camargo, "New fluorophosphate glasses co-doped with Eu^{3+} and Tb^{3+} as candidates for generating tunable visible light," J. Alloys Compd. **647**, 315–321 (2015).
43. W. D. A. M. de Boer, C. McGonigle, T. Gregorkiewicz, Y. Fujiwara, S. Tanabe, and P. Stallinga, "Optical excitation and external photoluminescence quantum efficiency of Eu^{3+} in GaN," Sci. Rep. **4**(1), 5235 (2015).
44. I. I. Kindrat and B. V. Padlyak, "Luminescence properties and quantum efficiency of the Eu-doped borate glasses," Opt. Mater. **77**, 93–103 (2018).
45. S. Babu and Y. C. Ratnakaram, "Emission characteristics of holmium ions in fluoro-phosphate glasses for photonic applications," AIP Conf. Proc. **1731**(1), 070001 (2016).
46. F. Huang, Y. Zhang, L. L. Hu, and P. D. Chen, "Judd–Ofelt analysis and energy transfer processes of Er^{3+} and Nd^{3+} doped fluoroaluminate glasses with low phosphate content," Opt. Mater. **38**, 167–173 (2014).
47. S. K. Gupta, N. Pathak, and R. M. Kadam, "An efficient gel-combustion synthesis of visible light emitting barium zirconate perovskite nanoceramics: probing the photoluminescence of Sm^{3+} and Eu^{3+} doped $BaZrO_3$," J. Lumin. **169**, 106–114 (2016).
48. Y. Jin, J. H. Zhang, and W. P. Qin, "Photoluminescence properties of red phosphor $Gd_3Po_7:Eu^{3+}$ for UV-pumped light-emitting diodes," J. Alloys Compd. **579**, 263–266 (2013).
49. G. Lakshminarayana, J. Qiu, M. G. Brik, G. A. Kumar, and I. V. Kityk, "Spectral analysis of Er^{3+}-, Er^{3+}/Yb^{3+}- and $Er^{3+}/Tm^{3+}/Yb^{3+}$-doped TeO_2-ZnO-WO_3-TiO_2-Na_2O glasses," J. Phys. Condens. Matter **20**(37), 375101 (2008).
50. X. Q. Xiang, B. Wang, H. Lin, J. Xu, J. M. Wang, T. Hu, and Y. S. Wang, "Towards long-lifetime high-performance warm w-LEDs: Fabricating chromaticity-tunable glass ceramic using an ultra-low melting Sn-PFO glass," J. Eur. Ceram. Soc. **38**(4), 1990–1997 (2018).
51. U. Caldiño, I. Camarillo, A. Speghini, M. Bettinelli, and T. B. De. Queiroz, "Down-shifting by energy transfer in Tb^{3+}/Dy^{3+} co-doped zinc phosphate glasses"," J. Lumin. **161**, 142–146 (2015).
52. C. R. Kesavulu, K. K. Kumar, N. Vijaya, K. S. Lim, and C. K. Jayasankar, "Thermal, vibrational and optical properties of Eu^{3+}-doped lead fluorophosphate glasses for red laser applications," Mater. Chem. Phys. **141**(2–3), 903–911 (2013).
53. M. V. V. Kumar, B. C. Jamalaiah, K. R. Gopal, and R. R. Reddy, "Novel Eu^{3+}-doped lead telluroborate glasses for red laser source applications," J. Solid State Chem. **184**(8), 2145–2149 (2011).
54. W. Stambouli, H. Elhouichet, B. Gelloz, and M. Férid, "Optical and spectroscopic properties of Eu-doped tellurite glasses and glass ceramics," J. Lumin. **138**(6), 201–208 (2013).
55. L. G. Dai, L. Wang, H. Q. Jia, W. X. Wang, J. M. Zhou, W. M. Liu, and H. Chen, "Realization of high-luminous-efficiency InGaN light-emitting diodes in the "green gap" range," Sci. Rep-UK. **5**, 10883 (2015).
56. D. G. Li, W. P. Qin, S. H. Liu, W. B. Pei, Z. Wang, P. Zhang, L. L. Wang, and L. Huang, "Synthesis and luminescence properties of RE^{3+} (RE= Yb, Er, Tm, Eu, Tb)-doped Sc_2O_3 microcrystals," J. Alloys Compd. **653**, 304–309 (2015).
57. J. Rajagukguk, J. Kaewkhao, M. Djamal, R. Hidayat, and Y. Ruangtaweep, "Structural and optical characteristics of Eu^{3+} ions in sodium-lead-zinc-lithium-borate glass system," J. Mol. Struct. **1121**, 180–187 (2016).
58. L. Li, H. T. Lin, S. T. Qiao, Y. Zou, S. Danto, K. Richardson, J. D. Musgraves, N. S. Lu, and J. J. Hu, "Integrated flexible chalcogenide glass photonic devices," Nat. Photonics **8**(8), 643–649 (2014).
59. X. M. Zang, D. S. Li, E. Y. B. Pun, and H. Lin, "Dy^{3+} doped borate glasses for laser illumination," Opt. Mater. Express **7**(6), 2040–2054 (2017).